

The Influence of Deck Flexibility on the Dynamic Response of Railway Bridges

Pollyana Gil Cunha Amaral (1); Carlos Eduardo Nigro Mazzilli (2)

Abstract

A simplified methodology is proposed for railway bridge vibration analysis under train loading. Dynamic models of both train and bridge were assumed to be initially uncoupled, yet bound by contact forces. These forces were evaluated from the dynamic response of the vehicle subjected to support excitation caused by rail and wheel geometric irregularities. Such forces were statically condensed in the vehicle centre of gravity and applied to a 3D-beam finite-element model of the bridge. The influence of the rigid-deck hypothesis on the dynamic response is assessed via an iterative procedure to redefine updated "equivalent rail irregularities" as the sum of the deck displacements and the "actual" rail irregularities. The new interaction forces are re-applied to the bridge model to determine new displacements, repeating the procedure until the results converge.

Keywords: Dynamic Analysis, Railway Bridges, Geometric Irregularities, Contact Forces, Iterative Procedure, Frequency-Domain Spectrum

1 Introduction

This work addresses the vibration analysis of railway bridges produced by a typical passenger train, or EUT (Electric Unit Train), running along them. To this goal, a simplified dynamic-analysis methodology is presented, which assumes, in an initial step, that the vehicle and the bridge structural models can be de-coupled to ease the determination of the contact forces. Yet, this approximate assumption will

http://dx.doi.org/10535/rsee.v13i3/6532

 $^{(1)\,}MSc,\,University\,of\,S\~{a}o\,Paulo-pollyanagca@gmail.com$

⁽²⁾ Professor, Escola Politécnica da University of São Paulo – cenmazzi@usp.br

Av. Prof. Almeida Prado, Trav. 2 número 83, Cidade Universitária, CEP: 05508-900, São Paulo, Brazil

be corrected at a later step by means of an iterative procedure that will be described herewith. It is meant that the methodology should be sufficiently accessible to structural engineers making use of commercial finite-element codes, widely available.

To obtain the dynamic contact forces, a fifteen-degree-of-freedom model of the vehicle is used, according to [1], namely bounce (vertical displacement), sway (transversal displacement), roll (rotation about the longitudinal axis), pitch (rotation about the transversal axis) and yaw (rotation about the vertical axis), for the wagon suspended mass and the two bogies. The sway and yaw degrees of freedom are of particular interest to excite flexural modes of the bridge deck in the horizontal plane, as well as horizontal reactions applied at the column top ends, of great relevance for the meso- and infra-structure analysis. Bounce and pitch, on their turn, are important when flexural modes of the bridge deck in the vertical plane are excited. Roll acts upon torsion modes of the bridge deck. Bounce, pitch and roll interact to produce vertical reactions applied to the top end of columns.

Geometric irregularities both in the rails and the wheels are the primary causes for the time variation of the contact forces. These irregularities will be modelled here by functions proposed in the literature, as seen in [2].

Both the vehicle and the bridge deck will be modelled by the finite-element code ADINA – *Automatic Dynamic Incremental Nonlinear Analysis* –, available at the Computational Mechanics Laboratory of Escola Politécnica, University of São Paulo.

The modal analyses of the vehicle model, with the aforementioned 15 degrees of freedom, and of the bridge-deck model are carried out, to start with. It should be mentioned that two finite-element bridge-deck models were considered at this point: a high-hierarchy one, with shell elements and a low-hierarchy 3D-beam elements. This latter one is meant to be used in the forced dynamical analysis, for the sake of simplicity, once the contact forces are determined. Yet, the comparison between the results of the modal analyses for both the high- and the low-hierarchy models is useful to validate the latter one, for the purpose of the simplified methodology. Next, under the assumption of rigid rails and wheels, although being imperfect, the vehicle dynamic response under the equivalent support excitation is carried out, which supplies the contact forces in all wheels. The contact forces are

then statically condensed at the vehicle centre of mass, thus leading to a movable "equivalent" five-degree-of-freedom loading system (bounce force, sway force, roll moment, pitch moment and yaw moment) that travels with a constant speed along the 3D-beam-element model.

The dynamic analysis of the 3D-beam-element model subjected to the travelling five-degree-of-freedom loading system follows next, leading to displacements and internal forces time histories.

An iterative procedure can now be devised, by re-defining the "equivalent" rail imperfections as the sum of the time functions of the original rail imperfections at a certain position and the deck displacements at the same position, at the same time. A new dynamic analysis of the vehicle would be made, leading to new contact forces that would be statically condensed at the vehicle centre of mass, which would be applied to the bridge deck model, and so on.

The dynamic response would hopefully converge after a few iterations.

2 Modelling

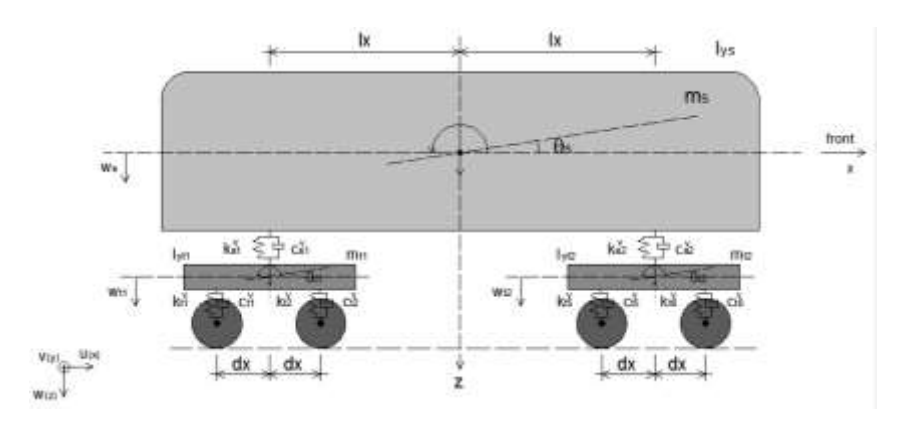
2.1 Vehicle model

As discussed above, the methodology considers a fifteen-degree-of-freedom model for the car. Since geometrical and mechanical for typical passenger wagons used in the Brazilian railways properties were not all available, it was considered here the vehicle of [3], whose parameters are shown in Table 1. Figure 1 illustrates the vehicle model.

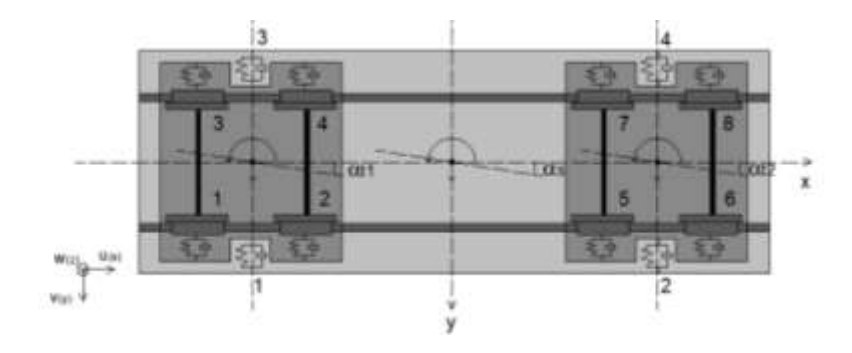
Table 1: Car mechanical and dynamic parameters (extracted from [3])

Parameter	Unit	Value
Wagon mass (m _s)	kg	50990
Wagon inertia moment of mass in roll (I_{xs})	kg.m²	1,55.10 ⁵
Wagon inertia moment of mass in pitch (Iys)	kg.m²	1,96.10 ⁶
Wagon inertia moment of mass in yaw (Izs)	kg.m²	1,88.10 ⁶
Bogie mass (m _t)	kg	4360
Bogie inertia moment of mass in roll (Ixt)	kg.m²	1,47.10 ³
Bogie inertia moment of mass in pitch (Iyt)	kg.m²	3,43.10 ³
Bogie inertia moment of mass in yaw (Izt)	kg.m²	5,07.10 ³
Primary-suspension vertical stiffness (k _t ^v)	kN/m	2976
Primary-suspension lateral stiffness (k _t ^h)	kN/m	20000
Secondary-suspension vertical stiffness (k _s ^v)	kN/m	1060
Secondary-suspension lateral stiffness (k _s ^h)	kN/m	460
Primary-suspension vertical damping (c _t ^v)	kNs/m	15
Primary-suspension lateral damping (c _t ^h)	kNs/m	15
Secondary-suspension vertical damping (c _s ^v)	kNs/m	30
Secondary-suspension lateral damping (c _s ^h)	kNs/m	30
Vehicle total length	m	22.5
Distance between bogies (2l _x)	m	15.6
Distance between axles (2d _x)	m	2.5
Distance l _z	m	0.98
Distance a _z	m	0.36
Distance b _z	m	0.07
Distance d _y	m	0.98
Distance l _y	m	1.12

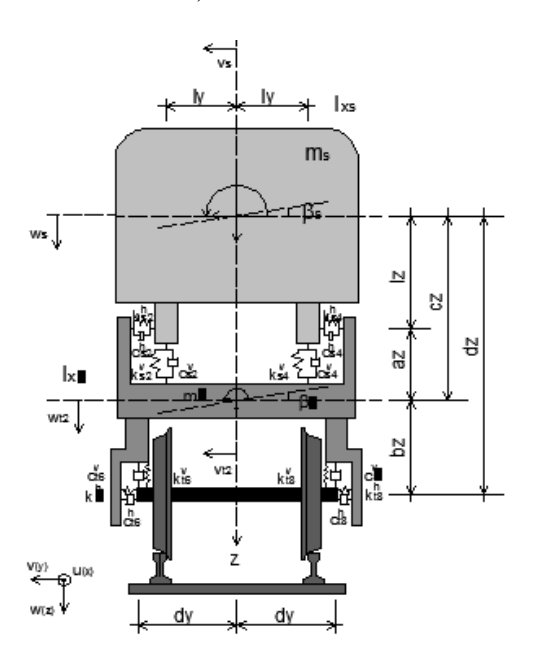
It is assumed that the train convoy is a composition of two EUT's, with four identical vehicles, totalling eight cars. Rigid links are used to connect the nodes where mass, damping and stiffness are positioned. The wheel masses are neglected and contact is assumed always. Figure 2 illustrates the vehicle model, as built in ADINA.



a) Longitudinal section



b) Horizontal section



c) Cross section

Figure 1: Vehicle model

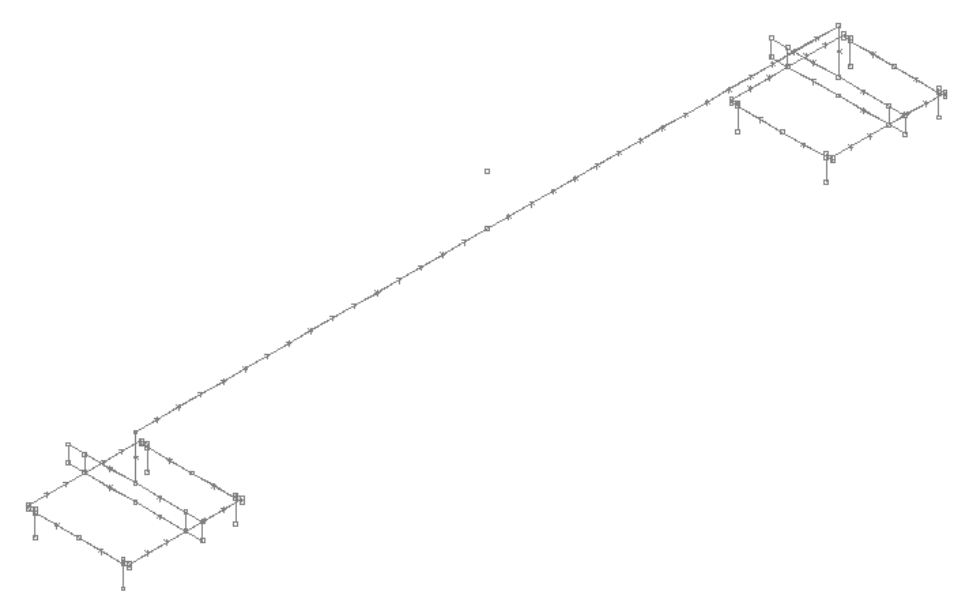


Figure 2: Vehicle model, as built in ADINA, showing rigid links (in brown) and springs and dampers (in green)

2.2 Rail and wheel geometric irregularities

The dynamic effect of the irregularities is to increase the load transferred to the bridge deck. It is assumed that rail irregularities, both in the vertical and horizontal planes, can be described by harmonic functions (Figure 3). They can induce significant vibration both in the vehicle and the bridge deck when its wavelength λ , crossed at a constant velocity V, will lead to a "forcing frequency" $\frac{2\pi V}{\lambda}$ close to a natural frequency of either structural system.

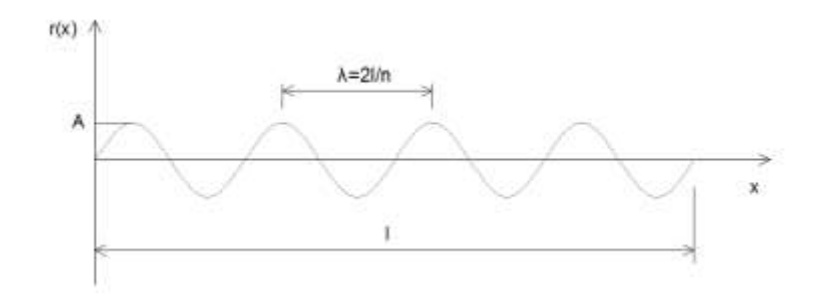


Figure 3: Simple harmonic irregularity

Phase differences between irregularities in the vertical and horizontal planes, as well as between the two rails, can be considered. Majka et al [4] stresses that the lateral dynamic response of a bridge is severely influenced by the rail

irregularities in the horizontal plane in straight spans, since centrifugal forces are not even present there.

As for the wheel geometric irregularities, localized notches can appear on the contact surface, due to the fact that the material of which they are made is less hard than the rail material.

The following functions are therefore used to model the irregularities, according to [2]:

a) Rail longitudinal irregularities:

$$r(x) = Asen\left(\frac{2\pi x}{\lambda} + \phi\right)$$
 (Eq. 1)

where:

A: irregularity amplitude in m;

x = Vt: distance travelled by the vehicle in m;

V: vehicle speed in m/s;

$$\lambda = \frac{2\ell}{n}$$
: wavelength in *m*;

 ℓ : length with irregularities in m;

n: number of irregularity half-waves ℓ ;

 ϕ : phase angle in *radians*.

In the present case study, irregularity amplitudes were assumed to be 5mm and 2mm, respectively in the vertical and horizontal planes. The phase angle was taken to be zero in the vertical plane and $\pi/2$ in the horizontal plane. Still with respect to the rail irregularities, the case n=5 was considered in both planes.

b) Wheel irregularities

The notches are modelled by the function depicted in Figure 4:

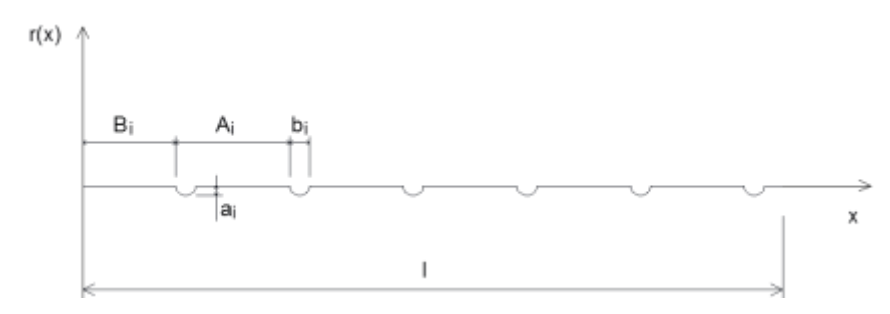


Figure 4: Wheel irregularity function

$$r(x) = \begin{cases} \frac{1}{2} a_i \left[1 - \cos \frac{2\pi}{b_i} (x - kA_i - B_i) \right], & \text{if} \quad B_i + kA_i \le x \le B_i + kA_i + b_i \\ 0, & \text{if} \quad B_i + kA_i + b_i < x < B_i + (k+1)A \end{cases}$$
 (Eq.2)

where:

 A_i , B_i , a_i e b_i : are indicated in Figu;

i : refers to the *i-th* wheel with notches;

k: 0, 1, 2...

The following notation is used in Figure 5:

A : circumference length in *m*;

B: distance of first wheel impact with respect to the bridge entrance in m;

a: notch depth in m;

b: notch length in m.

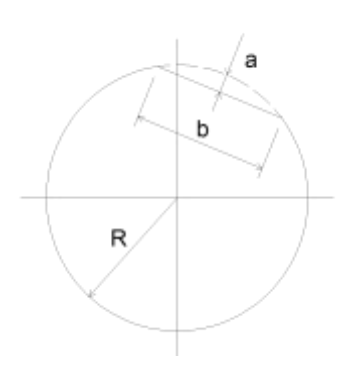
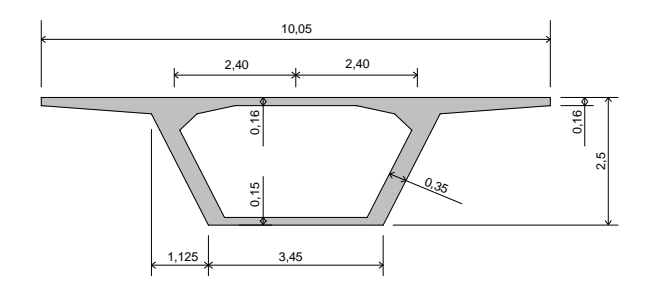


Figure 5: Wheel with a notch

2.3 Bridge-deck modelling

This case study refers to the bridge described in [5]. It is a 36m long reinforced-concrete bridge, for two tracks, so that the eccentricity of each track with respect to the deck longitudinal axis is 2.4m. It was chosen because its box-girder cross section allows for an easy 3D-beam model, as wished here. Geometric and mechanical properties are supplied in Figure . Figure shows a high-hierarchy model built in ADINA, which was used only for the modal analysis.



A	4.56	m²
Ix	3.52	m ⁴
Iy	28.88	m ⁴
It	6.68	m ⁴
Е	2.38x10 ¹⁰	N/m²
m	11169.84	kg/m
Ir _x	39273.16	kg.m²
Ir _y	1134090.97	kg.m²
E m Ir _x	2.38x10 ¹⁰ 11169.84 39273.16	N/m² kg/m kg.m²

Figure 6: Deck cross section and properties

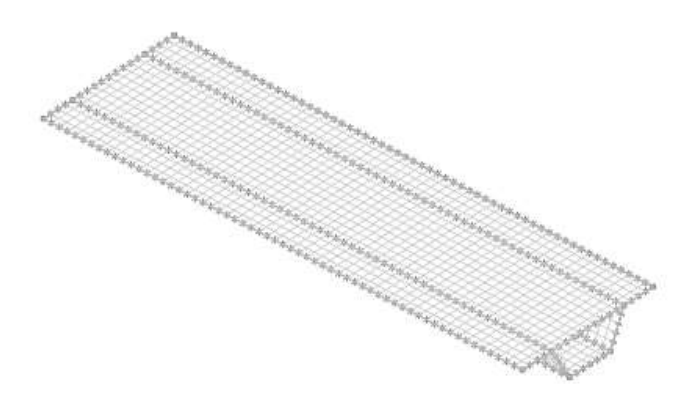


Figure 7: Shell-element finite-element model used in modal analysis

2.4 Reduced-order model for the contact forces and the bridge deck

As mentioned before, the reduced-order model for the contact forces comes out of the static condensation at the vehicle centre of mass, considering the set of all wheel-rail contact forces. It was assumed here that the train convoy travels at a constant speed V=20m/s. Therefore, the five-degree-of-freedom loading system (bounce force, sway force, roll moment, pitch moment and yaw moment) shown in Figure 8 also runs at the same speed along the 3D-beam model.

The structural damping was assumed to be of the Rayleigh type, with a modal damping ratio of 3% for the first and fifth natural modes, (natural frequencies 3.31Hz and 16.30~Hz, respectively), both of bending in the vertical plane.

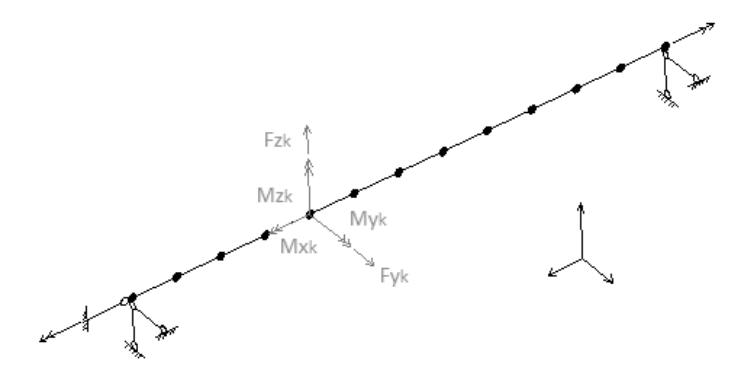


Figure 8: Loading of the 3D-beam model, as proposed by the simplified methodology

3 Results and concluding remarks

Table 2 displays the results of the modal analysis for both the vehicle and the bridge deck (with the high-hierarchy model). It should be mentioned that a good agreement was obtained between the analyses of the high- and low-hierarchy models, as far as the first relevant flexural modes are concerned. The scenario with n=5 (number of half-waves in the rail irregularity function) was chosen because, with a speed of V=20m/s, it leads to a dominant forcing frequency in the bounce force of 1,33Hz, which is approximately equal to the vehicle fourth mode of vibration. Thus, although this frequency is not resonant with respect to the bridge deck, it is with respect to the vehicle and leads to larger amplitude bounce-force. The reverse situation is, in principle, also worth of a study. That is, taking n=11,7 the bounce force will be almost resonant with the deck first vertical plane mode $(3,31\ Hz)$, yet away from resonances in the vehicle, which means that the amplitude of the bounce force is not as large, although applied at a more dangerous frequency for the bridge. It can be seen that, here, the scenario n=5 is more critical and that was the reason to choose it here.

Table 2: Natural frequencies

M-J	Deck Frequencies	Vehicle
Modes	[Hz]	Frequencies [Hz]
1°	3.307	0.645
2°	10.460	1.215
3°	10.560	1.230
4°	14.970	1.334
5°	16.300	1.667
6°	16.730	9.044
7°	17.410	9.055
8°	17.670	11.720
9°	18.160	11.720
10°	18.480	15.480
11°	18.830	15.480
12°	20.000	21.960
13°	21.600	21.960
14°	21.970	24.990
15°	22.620	24.990

The contact forces determined with the assumption of rigid deck are shown in Figure 9. It should be mentioned that these forces correspond to the steady-state portion of the diagrams shown in Figure 9 and that the dominant forcing frequency is 1.33~Hz, coinciding with the frequency of the fourth mode of vibration of the vehicle.

Once the contact forces are available, they can be applied to the 3D-beam model to carry out the dynamics analysis (transient analysis in ADINA), thus supplying displacements and internal forces as time histories. It is to be recalled here, that the deck response was obtained under the assumption of a rigid structure under the rails, which is not precise, since displacements did occur in the deck and were even estimated when the contact forces were applied to the structural model.

It is precisely to evaluate how good or bad was the assumption of a rigid structure to obtain the contact forces, that an iterative procedure is followed here to make new and better estimates of the contact forces and of the deck displacements. This is how it goes:

1st step: determination of the deck displacements for the contact forces with rigid structure underneath (this is already an available output!);

 2^{nd} step: deck displacements obtained in 1^{st} step are added to the rail irregularity functions, at each position x=Vt along the bridge and each time t, to produce an "equivalent irregularity" function;

3rd step: new contact forces are obtained from the dynamic analysis of the vehicle, under support excitation provided by the "equivalent irregularity" function of 2nd step;

4th step: determination of the deck displacements for the contact forces of 3rd step;

 5^{th} step: deck displacements obtained in 4^{th} step are added to the rail irregularity functions, at each position x=Vt along the bridge and each time t, to produce an "equivalent irregularity" function.

The procedure is repeated until convergence is achieved between the results of iterations "i" and "i-1".

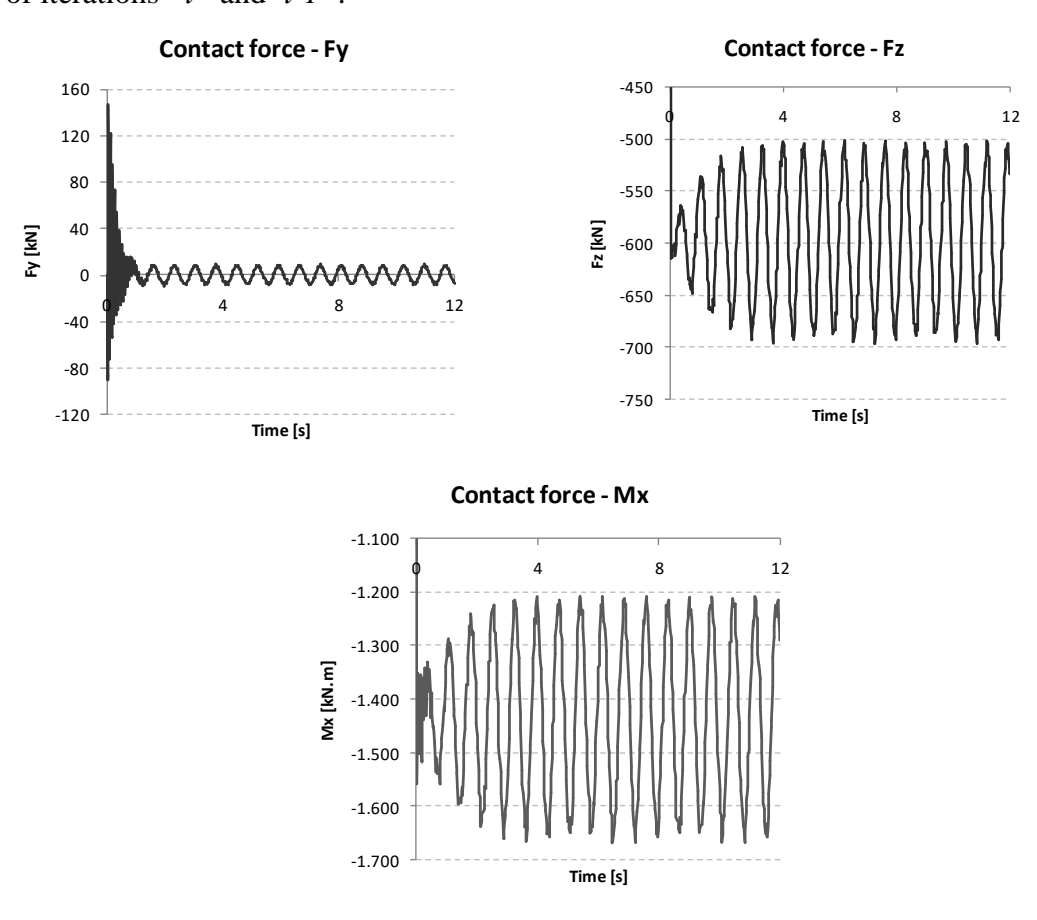


Figure 9: Contact forces – iteration i=0

In this case study, four iterations were carried out. For the sake of brevity, only the results of the "zero" and the fourth iteration are displayed, in Figure and Figure 4.

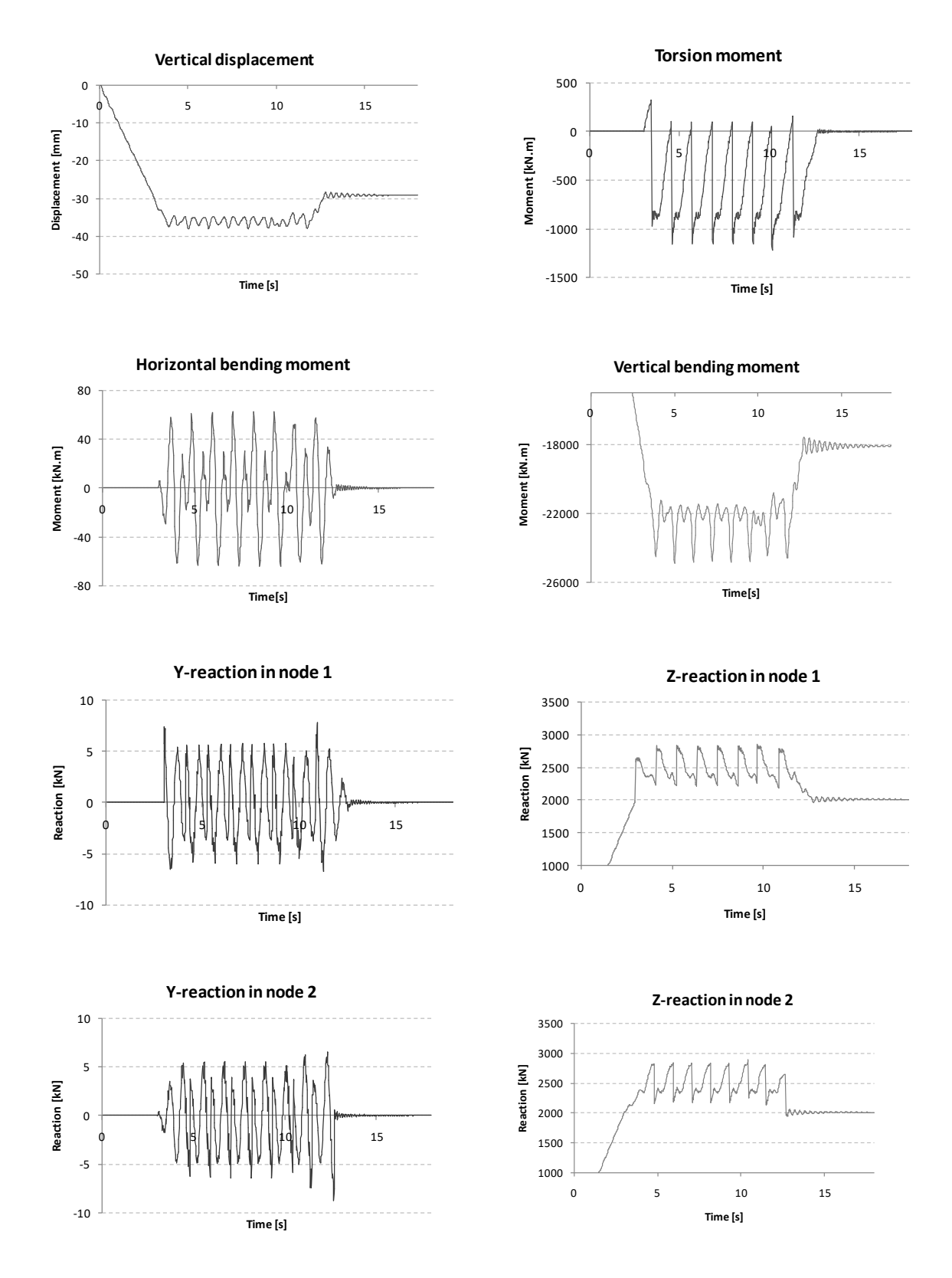


Figure 10: Results for iteration i=0 (contact forces for rigid structure)

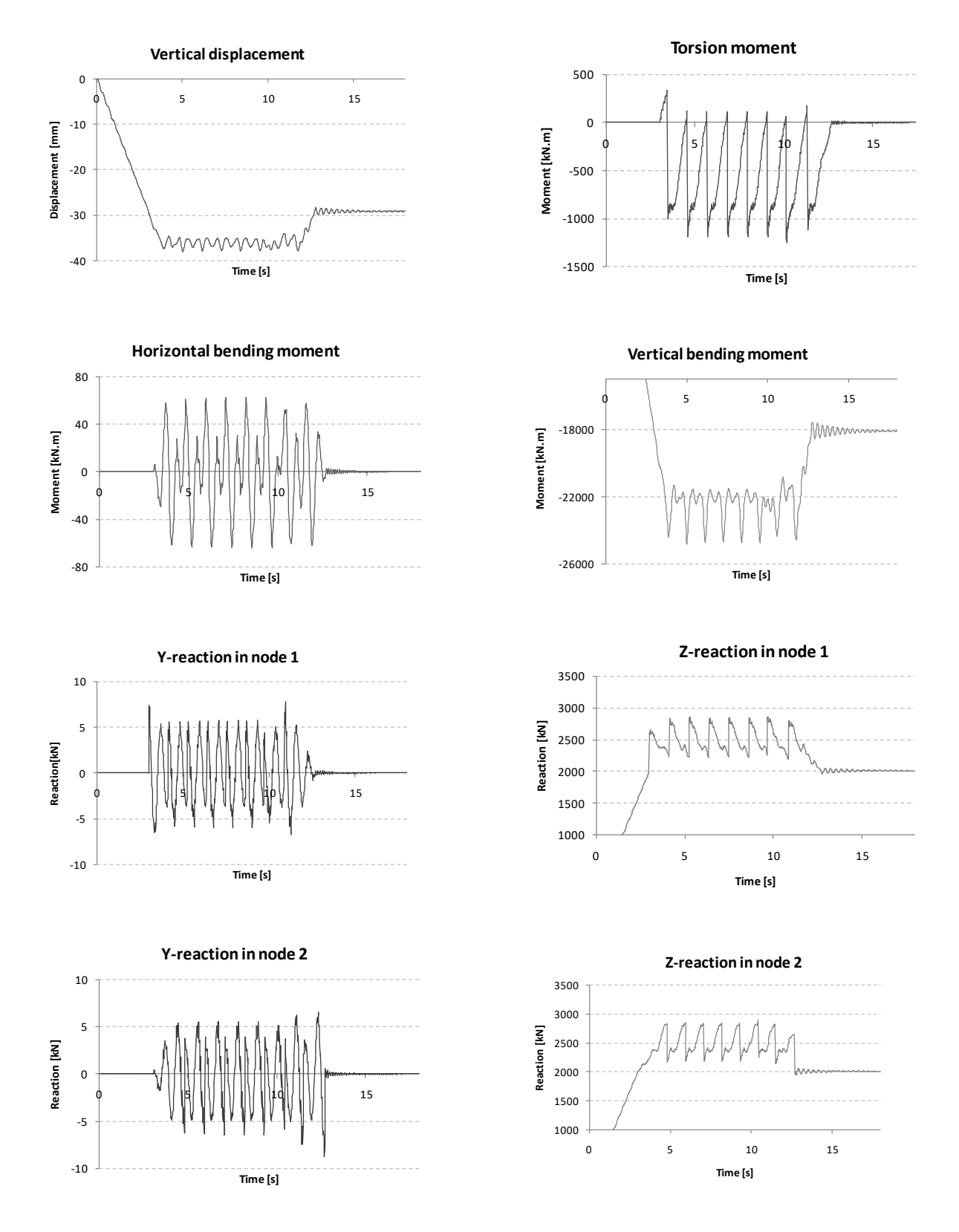


Figure 4: Results for iteration i=4

To check the iterative-procedure convergence, it was found useful to focus attention on the bounce force F_z , whose frequency-domain spectra are shown in Figures 12-16.

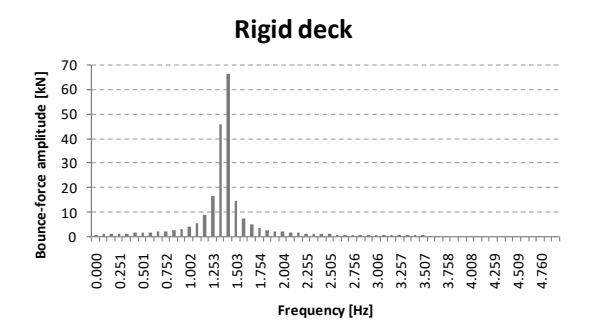


Figure 5: Frequency-domain spectrum for F_z – iteration i=0

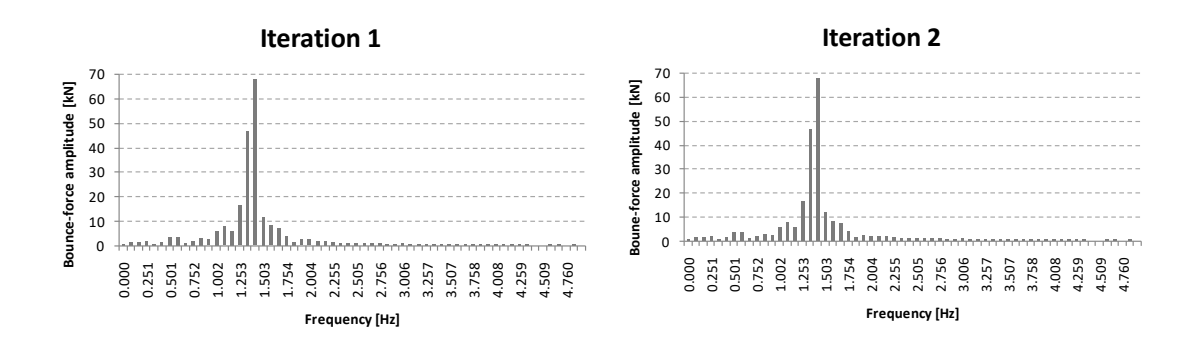


Figure 6: Frequency-domain spectrum for

 F_z – iteration i=1

for F_z —iteration i=2

Figure 7: Frequency-domain spectrum

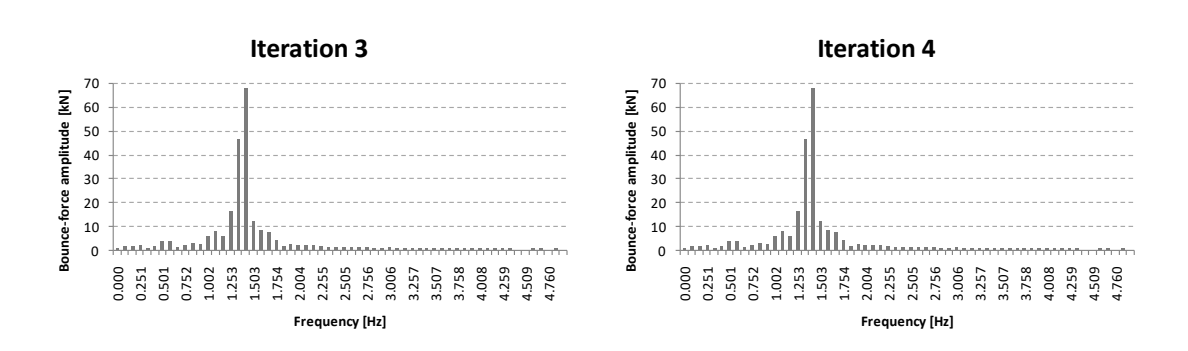


Figure 8: Frequency-domain spectrum for

Figure 9: Frequency-domain spectrum

 F_z —iteration i=3

for F_z – iteration i=4

Here, analogously to [6], the SRSS estimate, defined with respect to the spectra of Figures 12-16, is used to assess the deviations between any iteration i and the iteration i=0 (rigid structure assumption), as indicated in equation (3):

$$Deviation = \left(\frac{\sqrt{\sum_{w=1}^{60} A_{w,iteration(i)}^{2}}}{\sqrt{\sum_{w=1}^{60} A_{w,iteration(0)}^{2}}} - 1\right) 100\%$$
(Eq. 3)

Table 3 displays the computed deviations with respect to the iteration i=0 (rigid structure assumption) and also with respect to the previous iteration. It is readily noticed that after only four iterations the deviations with respect to the previous iteration were reduced to the order of 0.001%! Even more remarkable, are the very small deviations of all iterations with respect to the original hypothesis of rigid structure to evaluate the contact forces: in fact it is less than 2%, from the first iteration onwards. It could be said that in this case study the results for i=0 are sufficiently accurate for design purposes.

Table 3: Deviations between iterations (i,0) and (i,i-1)

Iteration	Deviation (i,0)%	Iteration	Deviation (i,i-1)%
0 - 1	1.934	0 - 1	1.934
0 - 2	1.883	1 - 2	-0.051
0 - 3	1.911	2 - 3	0.028
0 - 4	1.911	3 - 4	-0.001

Good matching is also observed between the estimates for displacements and internal forces of the structural model, when iteration i=4 is compared with i=0, as shown in Table 4:

Table 4: Results for the structural model (iterations i=0 and i=4)

Internal forces	Iteration 0	Iteration 4
Torsion moment	-1222.52	-1256.62
Horizontal bending moment	-64.04	-64.04
Vertical bending moment	-24912.90	-24831.80
Vertical displacement	-38.13	-38.01
Y-reaction in node 1	7.83	7.83
Y-reaction in node 2	-8.80	-8.80
Z-reaction in node 1	2851.86	2857.16
Z-reaction in node 2	2884.38	2890.30

References

- [1] P.G. Cunha (2011). "Análise Dinâmica de Pontes Ferroviárias: Uma Metodologia Simplificada. Dissertação de Mestrado", POLI/USP, São Paulo, SP, Brasil.
- [2] W.L. Correa (2008). "Controle das Vibrações Induzidas pela Interação Dinâmica entre Trens-Trilhos-Dormentes-Estrutura de Aço de Pontes Ferroviárias". Tese, COPPE/UFRJ, Rio de Janeiro, RJ, Brasil.
- [3] H. Xia, Y.L. Xu and T.H.T. Chan (2000). "Dynamic Interaction of Long Suspension Bridges with Running Trains", Journal of Sound and Vibration 237, 263-280.
- [4] M. Majka and M. Hartnett (2009). "Dynamic Response of Bridges to Moving Trains: A Study on Effects of Random Track Irregularities and Bridge Skewness", Journal Computers & Structures, 87, 1233-1252.
- [5] L.G. Clemente, L.A. Borges e F. Stucchi (1989). "Projeto de viaduto unicelular para pista dupla na extensão da linha Norte/Sul do Metrô de São Paulo", Anais do Primeiro Simpósio EPUSP de Estrutura de Concreto.
- [6] F.V. Moroz (2009). "Uma Metodologia para a Análise da Influência no Tráfego de Carros Pesados na Resposta Dinâmica de Pontes Rodoviárias". Dissertação de Mestrado, POLI/USP, São Paulo.